scientific reports

Check for updates

OPEN

Metformin combined with local irradiation provokes abscopal effects in a murine rectal cancer model

Mineyuki Tojo[1], Hideyo Miyato[1], Koji Koinuma[1], Hisanaga Horie[1], Hidenori Tsukui[1], Yuki Kimura[1], Yuki Kaneko[1], Hideyuki Ohzawa[1], Hironori Yamaguchi[2], Kotaro Yoshimura[3], Alan Kawarai Lefor[1], Naohiro Sata[1] & Joji Kitayama[1]✉

Although preoperative chemoradiation therapy can down-stage locally advanced rectal cancer (LARC), it has little effect on distant metastases. Metformin exerts an anti-cancer effect partly through the activation of host immunity. LuM1, a highly lung metastatic subclone of colon 26, was injected subcutaneously (sc) in BALB/c mice and treated with metformin and/or local radiation (RT). Lung metastases and the primary tumors were evaluated and the phenotypes of immune cells in the spleen and lung metastases were examined with flow cytometry and immunohistochemistry. Local RT, but not metformin, partially delayed the growth of sc tumor which was augmented with metformin. Lung metastases were unchanged in metformin or RT alone, but significantly reduced in the combined therapy. The ratios of splenic T cells tended to be low in the RT group, which were increased by the addition of metformin. IFN-γ production of the splenic CD4(+) and CD8(+) T cells was enhanced and CD49b (+) CD335(+) activated NK cells was increased after combined treatment group. Density of NK cells infiltrating in lung metastases was increased after combination treatment. Metformin effectively enhances local and abscopal effects of RT though the activation of cell-mediated immunity and might be clinically useful for LARC.

Neoadjuvant radiotherapy (RT) and systemic chemotherapy can induce downstaging of locally advanced rectal cancer (LARC) leading to reduced local recurrence rates[1–3] and is now considered standard treatment for patients with LARC worldwide[4,5]. However, the incidence of distant metastases is not decreased, and many radiosensitizers have been examined in clinical trials to improve the efficacy and tolerability of RT.

Metformin is an oral antihyperglycemic drug used as first-line treatment for some patients with type 2 diabetes mellitus for over 50 years. Numerous epidemiologic studies have suggested that metformin use can significantly reduce the incidence of cancer development and mortality among patients with type 2 diabetes mellitus, although the rate of reduction differs for various types of cancer[6–11]. Numerous studies have demonstrated that metformin enhances DNA damage of tumor cells via multiple mechanisms which can exert radiosensitizing effects[12–17]. Since metformin has been widely prescribed because of its well-known safety profile and low cost, many clinical studies have already been conducted. Some of these studies have shown that metformin improves outcomes in patients who received RT for the treatment of various cancers including colorectal cancer[18–22]. However, synergistic effects of these two treatment modalities were not always evident[23–25] and detailed molecular mechanisms of the synergism are still unclear.

Generally, it is believed that RT induces transient immunosuppression. However, multiple reports have suggested that tumor cells which are dead or dying after treatment with RT can present tumor-associated antigens to host immune cells and evoke innate and adaptive immune responses[26,27]. Therefore, many preclinical studies have been conducted on the synergistic effects between RT and immunotherapy using immune checkpoint inhibitors, which suggest that the anti-tumor effects of RT are further enhanced by the concurrent administration of antibodies to CTLA-4 and PD-1[28–30]. Some clinical trials also have suggested synergistic effects between RT and

[1]Department of Gastrointestinal Surgery, Jichi Medical University, Yakushiji 3311-1, Shimotsuke, Tochigi 329-0498, Japan. [2]Department of Clinical Oncology, Jichi Medical University, Shimotsuke, Tochigi, Japan. [3]Department of Plastic Surgery, Jichi Medical University, Shimotsuke, Tochigi, Japan. ✉email: kitayama@jichi.ac.jp

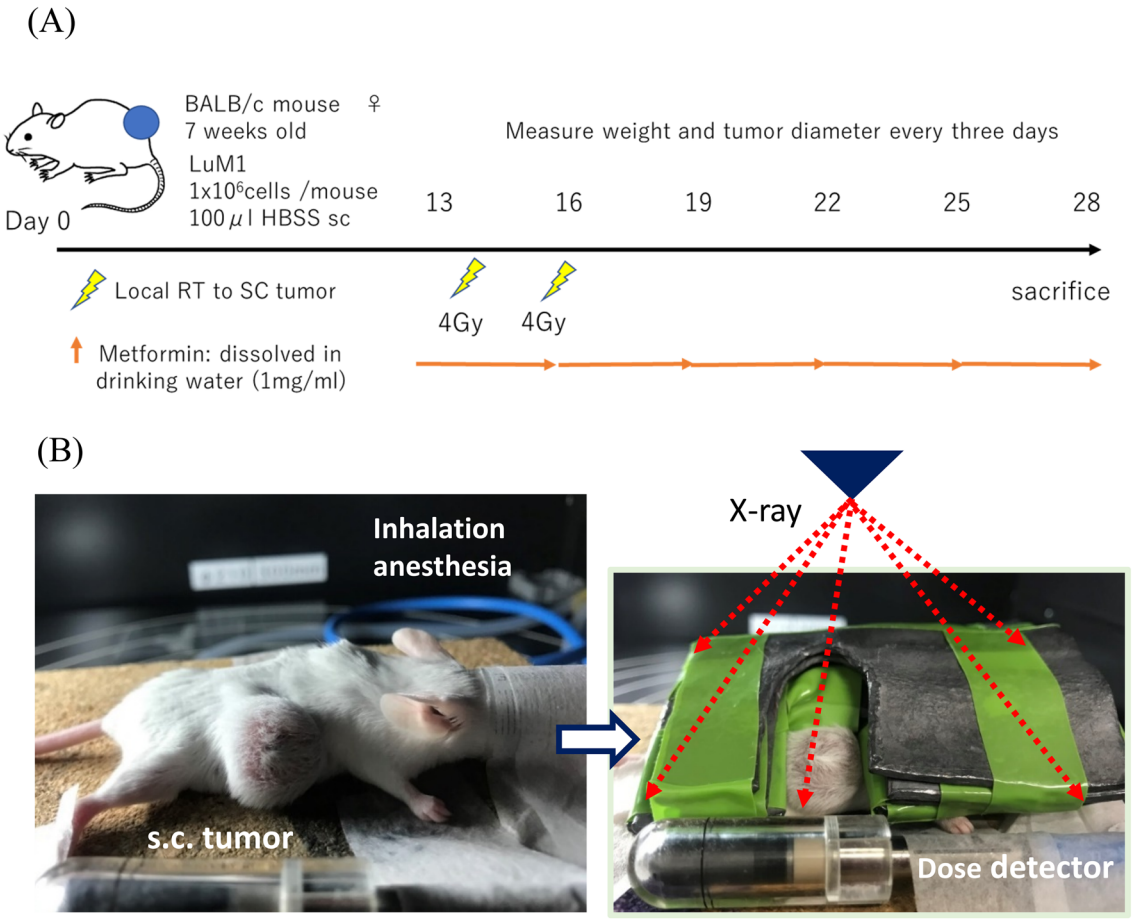

Figure 1. Treatment with radiation therapy (RT) and/or metformin. LuM-1 cells (1×10^6 per mouse) were subcutaneously injected in the right flank of 6–7 week-old female BALB/c mice. Local RT was delivered using MX 160 Labo (mediXtec, Chiba, Japan), as described in Materials and Methods. Metformin was dissolved in the drinking water (1 mg/mL) and administrated continuously from day13.

recently approved antibodies against PD-1 and CTLA-4[31,32]. However, such benefits have not been confirmed in other clinical studies[33,34], and the nature of agents which optimize responses to RT remain to be elucidated.

Recent studies have demonstrated that metformin loses its anti-tumor effects in severe combined immunodeficiency mice, suggesting the critical role of lymphocytes for these anti-tumor effects[35,36]. Metformin has also been shown to mediate the repolarization of macrophages from the M2 to M1 phenotype in the tumor microenvironment, which may lead to the inhibition of tumor growth in murine models[37–39]. More recently, metformin has been shown to downregulate programmed cell death receptor ligand-1 (PD-L1) in tumor cells[40–42] as well as to suppress the transcription of PD-1 gene in cytotoxic T cells (CTL)[43]. These experimental results suggest that the anti-tumor property of metformin is closely related to the host immune system.

In this study, a murine model of spontaneous lung metastases from colorectal cancer was used and the effects of combined local RT and systemic metformin on non-irradiated lung metastases examined, as well as on the irradiated subcutaneous tumor, focusing on effects on the host immune system (Fig. 1).

Results

Metformin augments the suppressive effects of RT on the growth of sc tumors. Subcutaneous tumors were observed in all mice about 10 days after sc injection and treatment started from day 13. Weight did not show significant differences in all groups (Fig. 2A). As shown in Fig. 2B,C, local RT (4 Gy × 2) suppressed the growth of sc tumors to a size approximately half that observed in the no treatment group although not statistically significantly ($p = 0.067$). Metformin alone did not significantly suppress tumor growth. However, when combined with RT, tumor weight at day 28 was significantly reduced compared with no treatment group ($p < 0.01$, n = 10).

Combined RT and metformin treatment suppressed the growth of non-irradiated lung metastases. The number of macroscopic metastases in non-irradiated lungs was counted after sacrifice on day 28. As shown in Fig. 3, multiple metastases developed in the lungs of mice in the no treatment group (median (M) = 120, 22–188) which was not significantly changed by treatment with metformin alone. The number of metastases tended to be reduced in the RT treated group, although not statistically significantly so (M = 34, 3–78,

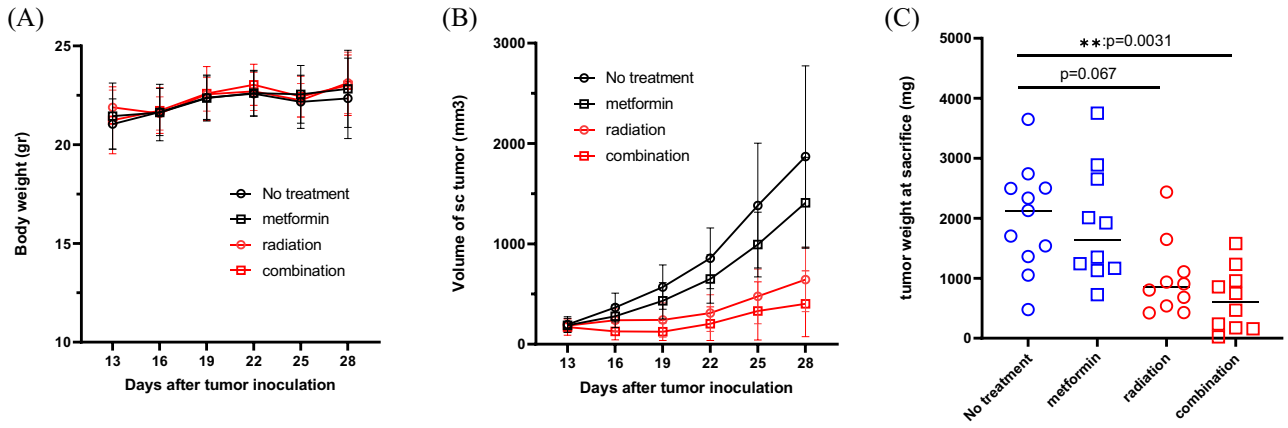

Figure 2. Mouse body weight (**A**) and tumor volume (**B**) were measured once every 3 days after the initiation of treatment. Mice were sacrificed on day 28 and the weight of subcutaneous tumors measured (**C**). The combined data of the results of 2 experiments (n = 5 in each) are shown: $^{**}p < 0.01$.

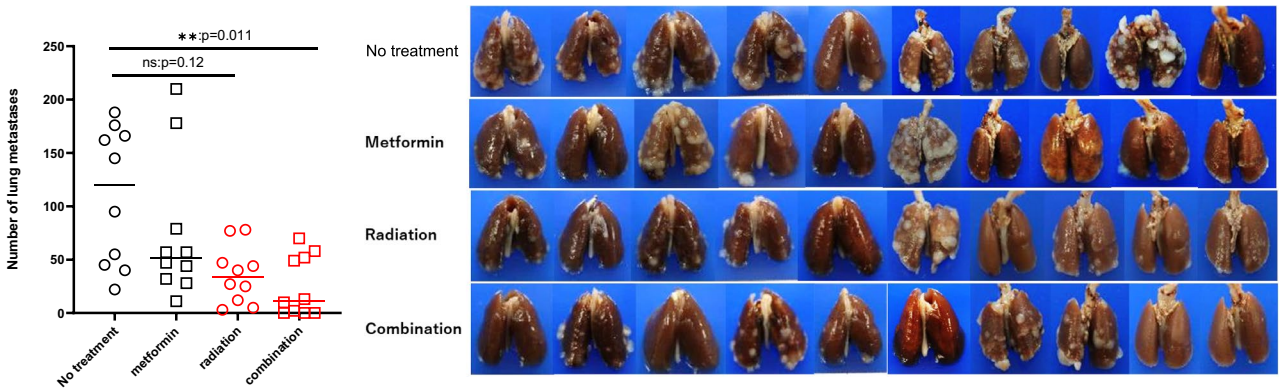

Figure 3. After sacrifice on day 28, the number of macroscopic metastatic nodules in the lungs evaluated. Data for the 2 experiments (n = 5 in each) are shown: $^{**}p < 0.01$.

$p = 0.12$). In comparison, when metformin was combined with RT treatment, the number of lung metastases was significantly decreased (M = 13, 0–70) with no metastases detected in 3/10 mice (Fig. 3). We also examined the metastatic lesions including the microscopic tumors inside the lung using microscopic observation in representative coronal tissue sections, and found that lung metastases were also suppressed significantly by combination treatment (Supplementary Fig. 1).

Combined RT and metformin treatment increased the frequencies of T and natural killer (NK) cells in the spleens of LuM-1 bearing mice. As shown in Fig. 4A, the ratios of CD3(+) or CD4(+) T cells at day 28 tended to be reduced in mice treated with RT alone, which were recovered in mice treated with both RT and metformin. The difference between RT treated mice and the combined therapy group was statistically significant (CD3:17.8 ± 2.9% vs 26.5 ± 5.9%, $p < 0.05$; CD4:14.7% ± 1.5% vs 17.1 ± 3.8%, $p < 0.05$). The ratios of CD8(+) T cells also showed the same trend (4.6% ± 1.2% vs 7.1 ± 1.8%, p = 0.14). The rate of CD19(+) B was not different (Fig. 4B). However, the rate of activated NK cells was significantly increased in the combined therapy group (1.1% ± 0.34% vs 2.6% ± 1.0%, $p < 0.05$) (Fig. 4C). The ratios of regulatory T cells (T_{reg}) and granulocytic- or monocytic-myeloid derived suppressor cells in splenocytes did not show significant differences among the 4 groups (Fig. 5).

Combined radiation and metformin treatment restored T cell exhaustion in spleens of LuM-1 bearing mice. We next examined T cell exhaustion in splenocytes. Although the expression of a representative exhaustive marker, PD-1 did not change significantly in CD4(+) and CD8(+) T cells, the ratios of PD-1 (+) cells tended to be lower in the combined treatment group compared with RT alone treated group (CD4;15.4 ± 6.7% vs 9.4% ± 1.7%, $p = 0.11$ CD8; 5.4 ± 1.0% vs 4.2% ± 0.80%, $p = 0.22$) (Fig. 4D). After stimulation with PMA and Ca^{2+} ionophore, the ratios of IFN-γ (+) cells were significantly increased in mice treated with both RT and metformin compared with those in the control group (CD4; 6.8 ± 2.4% vs 10.4 ± 1.3%, $p < 0.05$; CD8; 24.1 ± 3.1% vs 40.4 ± 3.1%, $p < 0.01$) (Fig. 6).

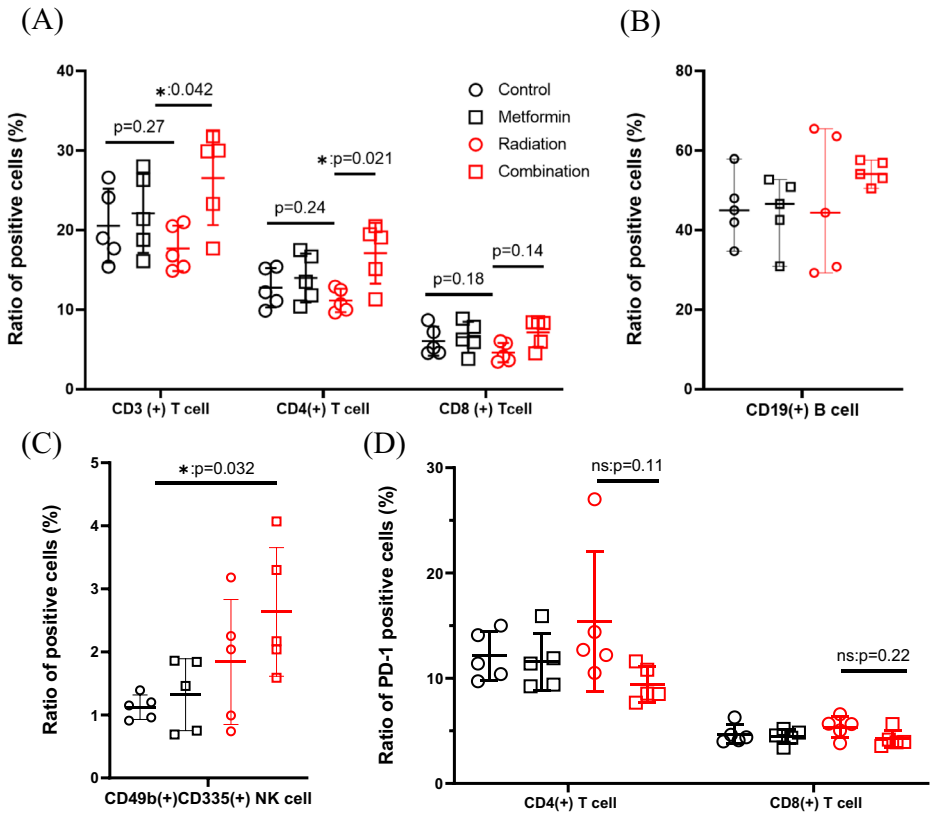

Figure 4. Splenocytes were harvested at day 28 and immunostained with mAbs to CD3, CD4, CD8, CD19and CD49b, CD335 and the frequencies of T (**A**), B (**B**) , activated NK (**C**) cells and PD-1(+) cells in CD4(+) or CD8(+) T cells (**D**) are determined in lymphocyte gate determined with flow cytometry. Data are shown as mean ± standard deviation of 5 mice in one of the 2 different experiments. $^{*}p < 0.05$.

The number of lung metastases correlates with the ratios of IFN-γ producing T and NK cells. Correlations between the character of splenocytes and lung metastases were examined in mice in the 4 groups. As shown in Fig. 7, the number of lung metastases was markedly reduced in mice with high ratios of IFN-γ of producing CD4(+) or CD8(+) T cells with Pearson correlation coefficients of − 0.58 and 0.63, respectively ($p = 0.0069$, 0.0029). Lung metastases showed the same inverse correlation with the frequency of CD49(+) CD335(+) NK cells ($r = -0.670$, $p = 0.0014$).

Combination therapy increased the density of NK cells while decreased the density of MDSC in lung metastases was decreased. The character of infiltrating immune cells in metastatic lesions larger than 40,000 μm^2 in lung tissue was evaluated with immunohistochemistry. The density of CD8a (+) cells was not changed among the 4 groups (Fig. 8B). However, as shown in Fig. 8A,C, the numbers of NKp46/CD335(+) NK cells in metastatic tumors were markedly increased only in mice treated with RT+ metformin compared with the no treatment group ($p < 0.0001$). In contrast, the density of Gr-1 (+) cells was significantly decreased in combined therapy treated group ($p = 0.012$) (Fig. 8A,D).

Discussion

Metformin has been shown to reduce the development of various malignancies and cancer-related mortality in patients with type 2 diabetes mellitus[6–10]. In patients with colorectal cancer, metformin has been shown to improve patient outcomes although the underlying mechanisms of how metformin exerts its anti-tumor effects are not fully understood[11,44–47]. Based on these observations, many preclinical studies were conducted to determine the clinical usefulness of combined RT and metformin which have had promising results[12,16,17]. However, the results of clinical studies are still inconsistent[21,22,25].

In previous in vivo studies[12,17], the anti-tumor effects of metformin on irradiated tumors were evaluated in immune deficient mice. However, recent studies have suggested that the anti-tumor effects of metformin are largely dependent on host immunity[35–39,43]. In this study, therefore, we used a syngeneic murine model of spontaneous lung metastases after sc implantation of colorectal cancer tumor cells and reevaluated the synergistic effects of combined RT and metformin.

LuM-1 is a highly aggressive and non-immunogenic subclone of colon 26[48], and metformin alone did not show significant anti-tumor effects on sc tumors or lung metastases. However, synergistic effects of RT and

metformin were observed. Selective RT (4 Gy × 2) delayed the growth of sc tumors with marginal statistical significance. However, when combined with oral metformin, the tumor suppressive effects of RT were markedly enhanced. More interestingly, combined therapy suppressed the growth of metastatic tumors in non-irradiated lungs. No metastases were detected in 3/10 mice. Metastatic lesions examined with tissue sections also show the same trends. The measurement of metastases with these methodologies may not be enough to assess the accurate total metastatic burden in lung. However, microscopic metastases from the primary LuM-1 tumor were already present in the lungs at the time of starting treatment[49], these data are highly suggestive that metformin not only enhances the cytotoxic effects on tumor cells directly exposed to RT but also causes tumor regression outside the irradiated field as a so-called "abscopal effect"[30,50].

Although DNA double-strand breaks in tumor cells are considered to be the primary mechanism of the anti-tumor effects of RT, recent studies suggest that a reduction in tumor size is also strongly dependent on immunogenic death of tumor cells mediated by T cell-mediated host immune responses after RT[51,52]. Indeed, local RT has been shown to increase the generation of tumor antigen-specific effector T cells in murine tumor models[52,53]. In data from the present study, the rates of CD3(+), CD4(+) and CD8(+) T cells tended to be decreased in the spleens of mice treated with RT alone presumably due to direct toxic effects of RT[54]. However, the ratios were significantly increased by the additional treatment with metformin. The frequencies of IFN-γ positive cells in CD4(+) and CD8(+) T cells were significantly elevated, and PD-1(+) cells in both T cell populations tended to be reduced in mice receiving combined therapy. The results observed in irradiated mice are consistent with those from previous studies showing that the anti-tumor effects of metformin result mostly from T cell mediated host immunity[35,36,43]. The IFN-γ producing activities of T cells is critical to suppress the growth of metastases since they inversely correlate with the degree of lung metastases in the mice in all 4 groups in the present study. Taken together, it is suggested that RT alone may reduce systemic T-cell mediated immunity associated with a non-immunogenic tumor such as LuM-1, while metformin restore T cell exhaustion which can efficiently induce abscopal effects.

Another interesting finding is that the frequency of activated NK cells defined by the CD49(+) CD335(+) phenotype showed a strong inverse correlation with the number of lung metastases and their ratios were significantly increased in mice treated with combined RT and metformin. Immunohistochemical analysis revealed that the number of CD335(+) activated NK cells, but not CD8(+) T cells, infiltrating metastatic lesions was increased in those mice. Consistent with this result, a recent study has demonstrated that metformin increases the frequency of CD335(+) NK cells in the spleen which suppresses pulmonary metastases from B16F10 melanoma[55].

However, infiltration of Gr-1(+) MDSC in lung metastases was reduced after combined treatment. Numerous studies have suggested that accumulation of MDSC provide a tumor permissive microenvironment through stimulation of angiogenesis as well as potent suppression of T cell functions[56,57]. MDSC have also been reported to inhibit NK cell functions[58–60], although the mechanistic interactions with NK cells are less clear than with T cells[61]. Considering the results of these studies, it is suggested that the abscopal effects induced by metformin and RT might be partially attributed to augmented NK cell activity caused by a reduced number of MDSC in the lung.

There is growing evidence that RT can result in in situ tumor vaccination by exposing tumor specific neoantigens to the host's innate immune system which then leads to immunogenic cell death of non-immunogenic tumor cells[51–53,62]. After successful results were found with immune check point inhibitors (ICI) in the treatment of various malignancies, radioimmunotherapy using the combination of RT and ICI has attracted much attention as an effective novel therapy for advanced malignancies. However, studies have shown conflicting results of the clinical usefulness of combined RT and ICI presumably due to differences in cancer immunogenicity as well as host immunity[31–34]. The present study shows that metformin efficiently enhances the abscopal effects of RT in non-immunogenic colorectal cancer tumors though the activation of T cell- and NK cell-mediated immunity. The results may not directly apply to humans. However, since metformin activates anti-tumor immunity by different mechanisms from anti-PD-1/PD-L1 or anti-CTLA-4 mAbs, the combination of immune check point inhibitors and metformin may provoke remarkable radiosensitizing effects leading to improved outcomes in patients with LARC.

Materials and methods

Reagents and antibodies. Metformin hydrochlorides was purchased from FUJIFILM-Wako Chemical (Osaka, Japan). Anti-mouse mAbs for flowcytometric analysis were used as described. FITC-conjugated anti-CD4(GK1.5), anti-CD8a(53-6.7), anti-CD49b(DX5), anti-Ly6c(HK1.4), and PE-conjugated anti-CD8a(53-6.7), anti-CD11c(N418), anti-CD19(6D5), anti-CX3CR1(SA0111F1), anti-IFN-γ (XMG1.2), and APC-conjugated anti-CD3(17A2), anti-CD11b(M1/70), anti-CD335(29A1.4), APC/Fire 750-conjugated anti-CD25(PC61), anti-CD45(30-F11), and BV421-conjugated anti-CD4(GK1.5), anti-FoxP3(MF-14), anti-Gr-1(RB6-8C5), anti-CD279(PD-1)(29F.1A12), and BV785-conjugated anti-CD45(30-F11), and pacific blue-conjugated CD45(30-F11) were purchased from BioLegend Inc. (San Diego, CA USA). FcR blocking reagent was purchased from Miltenyi Biotec B.V.& Co. KG (Bergisch Gladbach, Germany). FVS-780 and FVS-700 and Zombie UV were purchased from BD Biosciences (Franklin Lakes, NJ USA) and BioLegend Inc. (San Diego, CA USA), respectively. PMA and ionomycin, and Brefeldin A solution(1000X) were purchased from FUJIFILM (Osaka, Japan) and BioLegend Inc., (San Diego, CA USA), respectively. For Immunohistochemistry, mAbs to CD8a (4SM15, Rat IgG2a) and Ly-6G/Ly-6c (RB6-8C5, Rat IgG2b) were purchased from Invitrogen (Santa Clara, CA), and polyclonal Ab to NKp46/CD335 (EPR23097-35, Rabbit IgG) were from Abcam (Cambridge, MA).

Cell lines. LuM-1, a highly metastatic sub-clone of murine colon cancer, colon26[63] was kindly obtained from Dr. Oguri, Aichi Cancer Center, Japan, and maintained in RPMI supplemented with 10% FCS, 100 U/mL penicillin and 100 μg/mL streptomycin (Sigma-Aldrich, St. Louis, MO, USA). After achieving > 80% confluence, cells

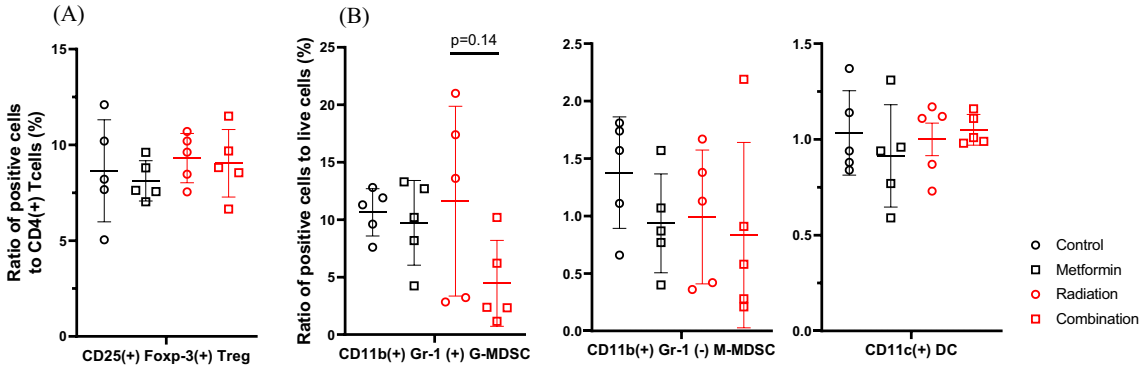

Figure 5. Splenocytes were harvested on day 28 and the frequencies of T-reg to CD4(+) T cell population (**A**) and CD11b(+)Gr-1(+) granulocytic-MDSC, CD11b(+)Gr-1(−) monocytic-MDSC as well as CD11c(+) DC in live cell gates (**B**) were determined with flow cytometry. Data are shown as mean ± standard deviation of 5 mice in one of the different 2 experiments.

were removed by treatment with TrypLE Express(Gibco), and then used for experiments. Cultured cells were tested using the Mycoplasma Detection Kit (R&D Systems, Minneapolis, MN, USA) every 3 months and used for experiments after three passages.

Animal model. The experimental protocol is shown in Fig. 1A. Female BALB/c mice 5–6 weeks old were purchased from CLEA Japan. (Tokyo, Japan) and housed in specific pathogen-free conditions. LuM-1 cells (1×10^6 per mouse) were injected subcutaneously in the right flank of 6–7 weeks-old female BALB/c mice. When the primary tumors reached a volume of 100–300 mm^3 at day13, mice were divided into four groups, each group containing 5–6 mice to enable statistical analysis (Group A, no treatment; Group B, metformin treated; Group C, radiation treated; Group D, metformin and radiation treated). Local RT was delivered using MX 160 Labo (mediXtec, Chiba, Japan), as described previously[49]. In short, anesthetized mice were held in the decubitus position, and radiation delivered only to the subcutaneous (sc) tumor with the remainder of the mouse including the lung covered with 3 lead plates with a thickness of 5 mm (Fig. 1B). We confirmed the X-ray was completely blocked by this apparatus. As a control, mice were similarly placed in the same conditions under anesthesia. Mice were administrated metformin hydrochloride (Wako) (1 mg/mL) or as indicated, dissolved in drinking water. Tumor diameter was measured with calipers and tumor volume calculated using tumor volume (mm^3) = [tumor length (mm) × tumor width $(mm)^2$]/2 and measured once every 3 days. Mouse weight was measured every 3 days. Mice were sacrificed using deep anesthesia by isoflurane on day 28, and the weight of the sc tumor and numbers of macroscopic metastatic nodules in the lungs were blindly evaluated by 2 investigators and average of the values were adopted. All procedures were approved by the Animal Care Committee of Jichi Medical University (No 19035-01) and performed in accordance with ARRIVE guidelines and the Japanese Guidelines for Animal Research.

Flow cytometry. For fluorescence activated cell sorting analysis, spleens were harvested and single cell suspensions prepared. After passing through 70 μm nylon mesh, red blood cells were eliminated with lysis buffer (NH4Cl, KHCO3, EDTA 4Na) and single cell suspensions prepared. Splenocytes were adjusted to $1X10^6$ cells in PBS containing 0.02% EDTA and incubated for 15 min to label dead cells. After washing with PBS, the cells were incubated with 5 μl FcR blocking reagent for 10 min and immunostained with relevant mAbs according to manufacturer's instructions. Intracellular staining of Foxp3 (BV421, BioLegend, clone MF-14) was performed using True-Nuclear Transcription Factor Buffer Set (BioLegend, San Diego, CA). After washing with PBS, the cell suspension was applied to BD LSRFortessaTM X-20 (Becton–Dickinson, San-Jose, CA USA) and antigen expression analyzed using Flow Jo TM software (Becton–Dickinson, San-Jose, CA USA). T cells producing IFN-γ were identified by intracellular staining. Prepared splenocytes (1×10^6) were cultured in RPMI-1640 + 10% FCS for 4 h at 37 °C in the presence of 50 ng/ml PMA (Wako Chemical) and 1 μg/ml ionomycin (Wako Chemical) and 5.0 μl/mL brefeldin A (BioLegend). The cells were harvested, fixed, permeabilized using the fixation and permeabilization solution (BD Bioscience) according to the manufacturer's instructions and stained with PE-conjugated IFN-γ or isotype control Rat IgG1 and FITC-conjugated anti-CD8a, APC-conjugated anti-CD3 and BV421-conjugated anti-CD4 mAb as well as FVS780 to exclude dead cells. The ratio of IFN-γ positive cells was calculated in CD3(+)CD4(+) or CD3 (+)CD8a (+) gated areas using LSR FortessaTM X-20 (BD Bioscience).

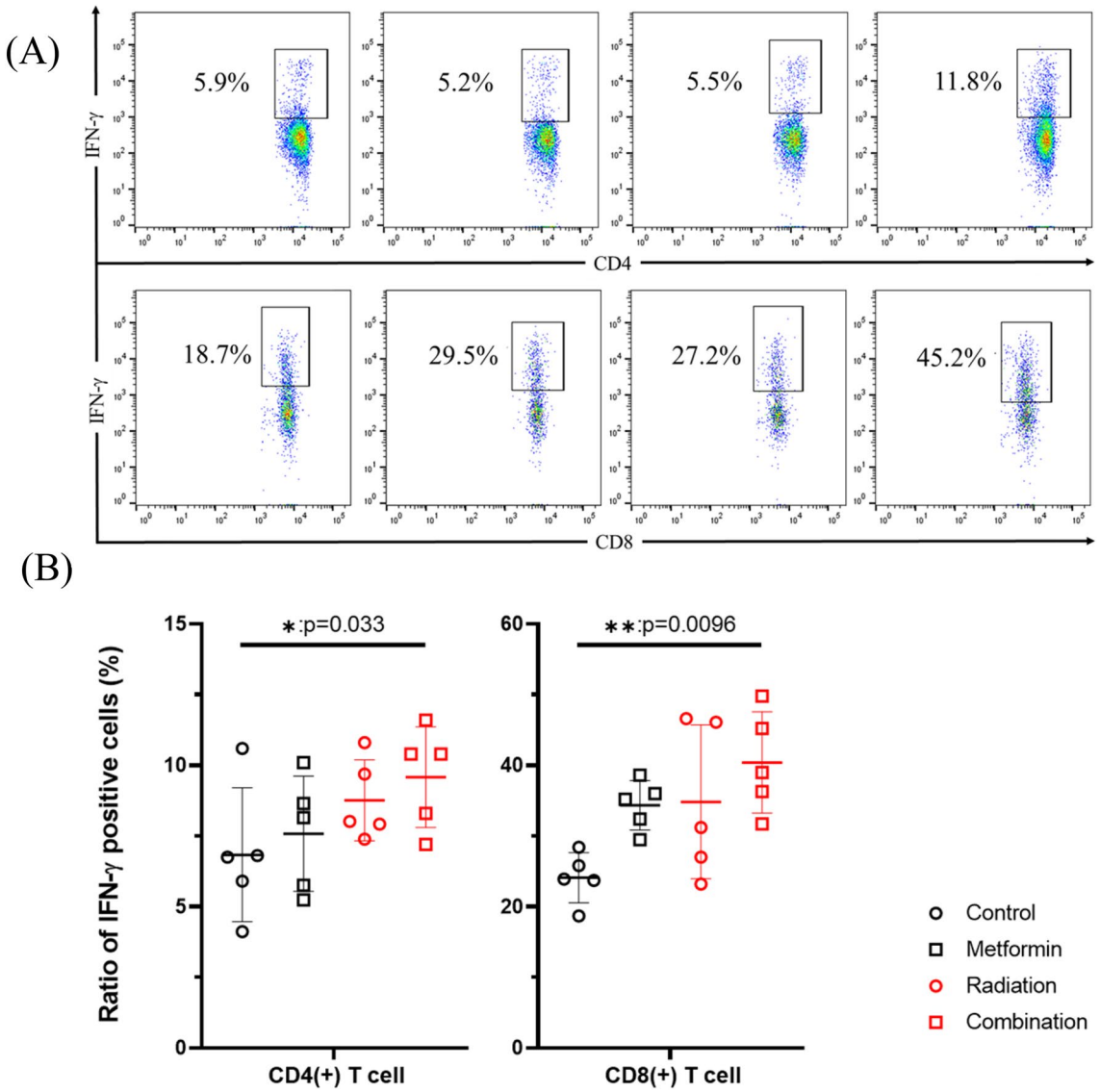

Figure 6. Splenocytes harvested on day 28 were cultured in the presence of 50 ng/ml PMA and 1 μg/ml ionomycin with 5.0 μl/mL brefeldin A for 4 h and cells positive for intracellular IFN-γ in these cell populations were evaluated with flow cytometry (**A**): Representative profiles of intracellular staining of IFN-γ (**B**) Data are shown as mean ± standard deviation of 5 mice in one of the 2 experiments. $^{*}p < 0.05$, $^{**}p < 0.01$.

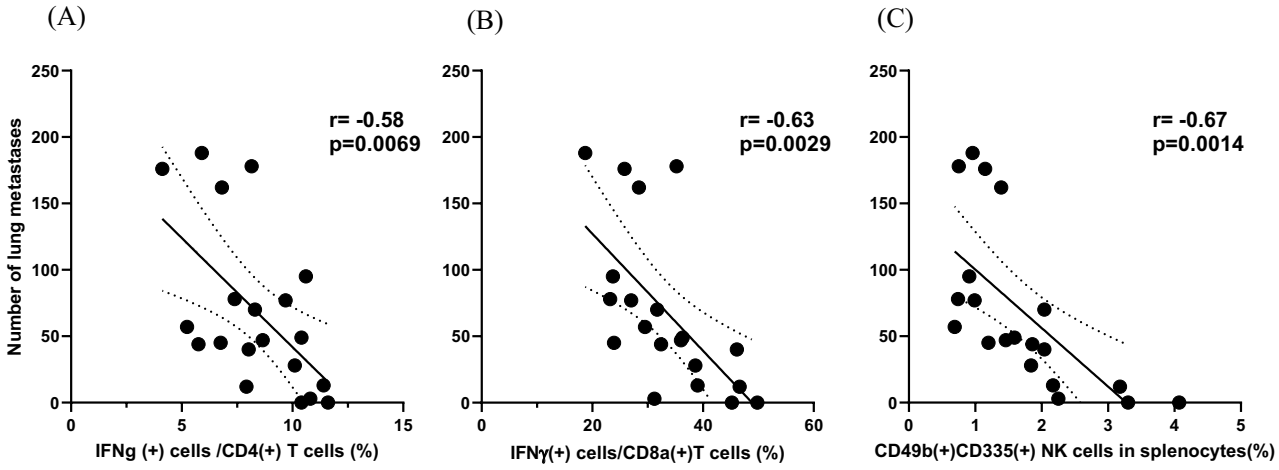

Figure 7. The correlation between the number of lung metastases and the ratios of IFN-γ (+) cells in CD4(+) (**A**) or CD8(+) T (**B**) cells as well as CD49b(+)CD335(+) NK (**C**) cells were evaluated with Pearson's correlation coefficients.

Immunohistochemistry of mice lung samples. Mice were sacrificed at day 28, lungs were internally fixed with 4% formalin, excised, and paraffin-embedded 4 μm sections were prepared for immunohistochemical evaluation. After endogenous peroxidase blocking by methanol and 30% hydrogen peroxide and heat-induced antigen retrieval in citrate buffer with microwaves, the specimens were incubated with 1% BSA for 30 min to block nonspecific antibody binding. Then, the slides were incubated with Abs to CD8a (at a dilution of 1:100), Ly-6G/Ly-6c (1:50), or NKp46/CD335 (1:500) in humid chambers overnight at 4 °C. After washings with PBS, sections were incubated with anti-rat or anti-rabbit secondary antibody conjugated with peroxidase for 30 min at room temperature. After washing, the enzyme substrate 3, 30-diaminobenzidine (Dako REAL EnVision Detection System, DAKO) was used for visualization and counterstained with Meyer's hematoxylin. In each tissue section, 1–5 different metastatic lesions larger than 40,000 μm^2 were randomly selected and positively stained cells were counted in those areas under the microscope. Thereafter, the densities of each cell type ($/mm^2$) were calculated using ImageJ software (NIH, Bethesda, MD).

Statistical analysis. For data on tumor volume, lung metastases and immunohistochemistry, *p*-values were evaluated with Kruskal–Wallis analysis followed by Dunn's multiple comparison tests. For splenocyte data, *p*-values were evaluated with one-way ANOVA followed by Tukey's honestly significant difference test. Correlation was examined with simple linear regression analysis. All analyses were performed with Graph Pad Prism 8 Software (San Diego, CA, USA), and p-values < 0.05 were considered statistically significant.

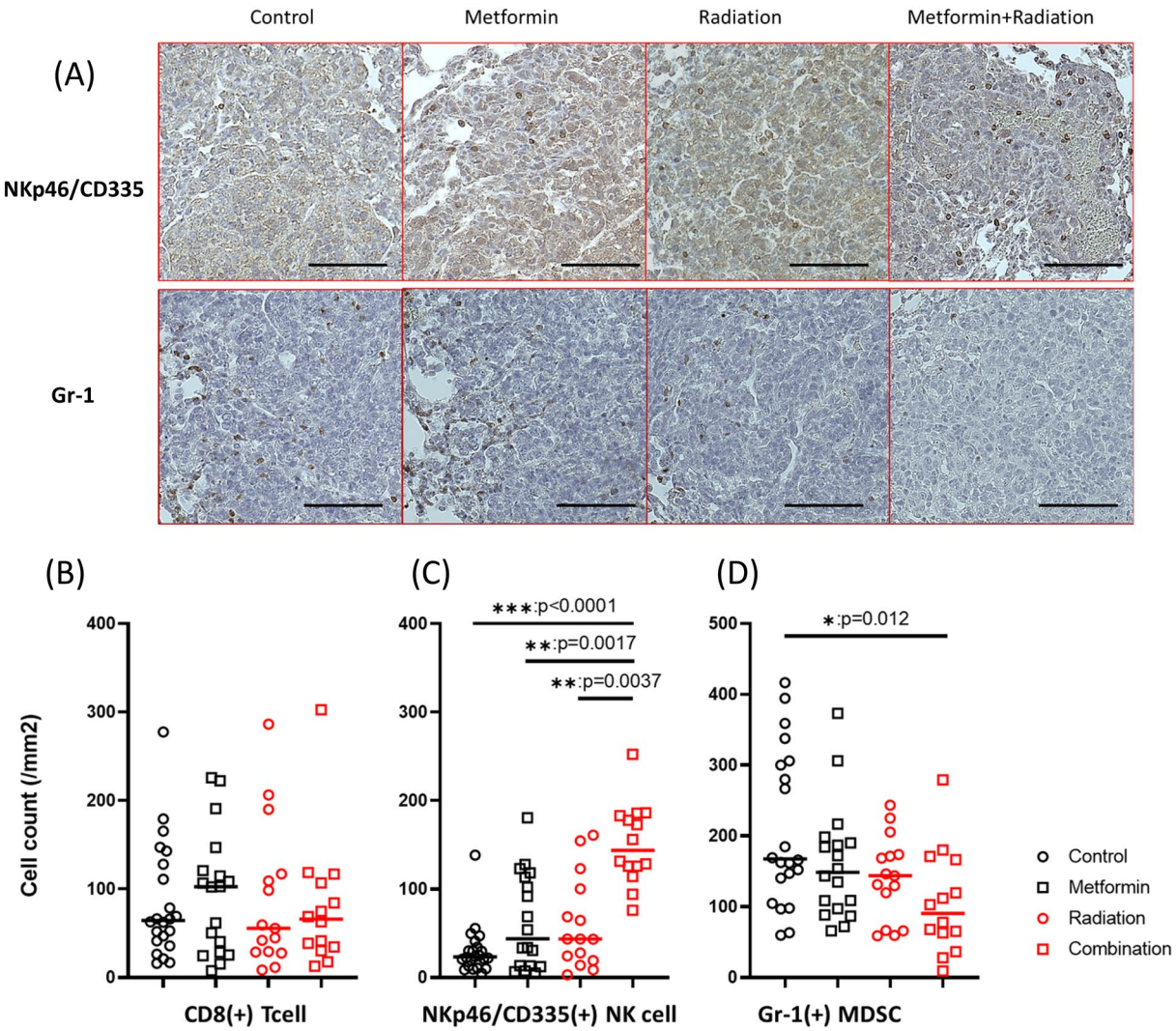

Figure 8. Immune cells in metastatic lesions in lung. Tissue specimens from the lungs excised at day 28 were immuno-stained with antibodies to CD8a, NKp46/CD335, or Gr-1(Ly-6G/Ly-6c) as described in Materials and Methods. (**A**) Representative immunohistochemistry of NKp46/CD335 (upper) and Gr-1 (lower) in metastatic lesions from the lung of the 4 groups. Black bars are 100 μm long. Densities of CD8(+) T cells (**B**), CD335(+) NK cells (**C**) and Gr-1(+) MDSC (**D**) infiltrating metastatic lesions in the lung. In each tissue section, the number of positively stained cells were determined in randomly selected 1–5 different metastatic lesions with more than 40,000μm^2 area using ImageJ software. (total: 22 lesions in control, 19 in metformin, 15 in RT and 14 in combination groups). *$p < 0.05$, **$p < 0.01$, ***$p < 0.001$.

Data availability

All data generated or analysed during this study were included in this published article and its supplementary information files.

Received: 17 December 2021; Accepted: 18 April 2022
Published online: 04 May 2022

References

1. Braendengen, M. *et al.* Randomized phase III study comparing preoperative radiotherapy with chemoradiotherapy in nonresectable rectal cancer. *J. Clin. Oncol.* **26**, 3687–3694. https://doi.org/10.1200/JCO.2007.15.3858 (2008).
2. Bosset, J. F. *et al.* Fluorouracil-based adjuvant chemotherapy after preoperative chemoradiotherapy in rectal cancer: Long-term results of the EORTC 22921 randomised study. *Lancet Oncol.* **15**, 184–190. https://doi.org/10.1016/S1470-2045(13)70599-0 (2014).
3. Bahadoer, R. R. *et al.* Short-course radiotherapy followed by chemotherapy before total mesorectal excision (TME) versus preoperative chemoradiotherapy, TME, and optional adjuvant chemotherapy in locally advanced rectal cancer (RAPIDO): A randomised, open-label, phase 3 trial. *Lancet Oncol.* **22**, 29–42. https://doi.org/10.1016/S1470-2045(20)30555-6 (2021).
4. Cellini, F. & Valentini, V. Current perspectives on preoperative integrated treatments for locally advanced rectal cancer: A review of agreement and controversies. *Oncology* **26**, 730–735 (2012).
5. Zheng, J., Feng, X., Hu, W., Wang, J. & Li, Y. Systematic review and meta-analysis of preoperative chemoradiotherapy with or without oxaliplatin in locally advanced rectal cancer. *Medicine* **96**, e6487. https://doi.org/10.1097/MD.0000000000006487 (2017).
6. Evans, J. M., Donnelly, L. A., Emslie-Smith, A. M., Alessi, D. R. & Morris, A. D. Metformin and reduced risk of cancer in diabetic patients. *BMJ* **330**, 1304–1305. https://doi.org/10.1136/bmj.38415.708634.F7 (2005).
7. Decensi, A. *et al.* Metformin and cancer risk in diabetic patients: A systematic review and meta-analysis. *Cancer Prev. Res.* **3**, 1451–1461. https://doi.org/10.1158/1940-6207.CAPR-10-0157 (2010).
8. Noto, H., Goto, A., Tsujimoto, T. & Noda, M. Cancer risk in diabetic patients treated with metformin: A systematic review and meta-analysis. *PLoS ONE* **7**, e33411. https://doi.org/10.1371/journal.pone.0033411 (2012).
9. Pollak, M. N. Investigating metformin for cancer prevention and treatment: The end of the beginning. *Cancer Discov.* **2**, 778–790. https://doi.org/10.1158/2159-8290.CD-12-0263 (2012).
10. Gandini, S. *et al.* Metformin and cancer risk and mortality: A systematic review and meta-analysis taking into account biases and confounders. *Cancer Prev. Res.* **7**, 867–885. https://doi.org/10.1158/1940-6207.CAPR-13-0424 (2014).
11. Dulskas, A. *et al.* Metformin increases cancer specific survival in colorectal cancer patients-National cohort study. *Cancer Epidemiol.* **62**, 101587. https://doi.org/10.1016/j.canep.2019.101587 (2019).
12. Zannella, V. E. *et al.* Reprogramming metabolism with metformin improves tumor oxygenation and radiotherapy response. *Clin. Cancer Res.* **19**, 6741–6750. https://doi.org/10.1158/1078-0432.CCR-13-1787 (2013).
13. Koritzinsky, M. Metformin: A novel biological modifier of tumor response to radiation therapy. *Int. J. Radiat. Oncol. Biol. Phys.* **93**, 454–464. https://doi.org/10.1016/j.ijrobp.2015.06.003 (2015).
14. Zhang, T. *et al.* Metformin sensitizes prostate cancer cells to radiation through EGFR/p-DNA-PKCS in vitro and in vivo. *Radiat. Res.* **181**, 641–649. https://doi.org/10.1667/RR13561.1 (2014).
15. Wang, Z. *et al.* Radiosensitization of metformin in pancreatic cancer cells via abrogating the G2 checkpoint and inhibiting DNA damage repair. *Cancer Lett.* **369**, 192–201. https://doi.org/10.1016/j.canlet.2015.08.015 (2015).
16. Jeong, Y. K., Kim, M. S., Lee, J. Y., Kim, E. H. & Ha, H. Metformin radiosensitizes p53-deficient colorectal cancer cells through induction of G2/M arrest and inhibition of DNA repair proteins. *PLoS ONE* **10**, e0143596. https://doi.org/10.1371/journal.pone.0143596 (2015).
17. Fernandes, J. M. *et al.* Metformin as an alternative radiosensitizing agent to 5-fluorouracil during neoadjuvant treatment for rectal cancer. *Dis. Colon Rectum* **63**, 918–926. https://doi.org/10.1097/DCR.0000000000001626 (2020).
18. Coyle, C., Cafferty, F. H., Vale, C. & Langley, R. E. Metformin as an adjuvant treatment for cancer: A systematic review and meta-analysis. *Ann. Oncol.* **27**, 2184–2195. https://doi.org/10.1093/annonc/mdw410 (2016).
19. Chevalier, B. *et al.* Metformin: (future) Best friend of the radiation oncologist?. *Radiother. Oncol.* **151**, 95–105. https://doi.org/10.1016/j.radonc.2020.06.030 (2020).
20. Oh, B. Y. *et al.* Metformin enhances the response to radiotherapy in diabetic patients with rectal cancer. *J. Cancer Res. Clin. Oncol.* **142**, 1377–1385. https://doi.org/10.1007/s00432-016-2148-x (2016).
21. Skinner, H. D. *et al.* Metformin use and improved response to therapy in rectal cancer. *Cancer Med.* **2**, 99–107. https://doi.org/10.1002/cam4.54 (2013).
22. Kim, J. M. *et al.* Survival benefit for metformin through better tumor response by Neoadjuvant concurrent chemoradiotherapy in rectal cancer. *Dis. Colon Rectum* **63**, 758–768. https://doi.org/10.1097/DCR.0000000000001624 (2020).
23. Tsakiridis, T. *et al.* Metformin in combination with chemoradiotherapy in locally advanced non-small cell lung cancer: The OCOG-ALMERA randomized clinical trial. *JAMA Oncol.* **7**, 1333–1341. https://doi.org/10.1001/jamaoncol.2021.2328 (2021).
24. Samsuri, N. A. B., Leech, M. & Marignol, L. Metformin and improved treatment outcomes in radiation therapy: A review. *Cancer Treat. Rev.* **55**, 150–162. https://doi.org/10.1016/j.ctrv.2017.03.005 (2017).
25. Planellas, P. *et al.* Is Metformin associated with improved response to neoadjuvant chemoradiotherapy in locally advanced rectal cancer?. *J. Surg. Res.* **268**, 465–473. https://doi.org/10.1016/j.jss.2021.06.079 (2021).
26. Gulley, J. L. *et al.* Combining a recombinant cancer vaccine with standard definitive radiotherapy in patients with localized prostate cancer. *Clin. Cancer Res.* **11**, 3353–3362. https://doi.org/10.1158/1078-0432.CCR-04-2062 (2005).
27. Golden, E. B. *et al.* Radiation fosters dose-dependent and chemotherapy-induced immunogenic cell death. *Oncoimmunology* **3**, e28518. https://doi.org/10.4161/onci.28518 (2014).
28. Dovedi, S. J. *et al.* Acquired resistance to fractionated radiotherapy can be overcome by concurrent PD-L1 blockade. *Cancer Res.* **74**, 5458–5468. https://doi.org/10.1158/0008-5472.CAN-14-1258 (2014).
29. Demaria, S., Golden, E. B. & Formenti, S. C. Role of local radiation therapy in cancer immunotherapy. *JAMA Oncol.* **1**, 1325–1332. https://doi.org/10.1001/jamaoncol.2015.2756 (2015).
30. Park, S. S. *et al.* PD-1 restrains radiotherapy-induced abscopal effect. *Cancer Immunol. Res.* **3**, 610–619. https://doi.org/10.1158/2326-6066.CIR-14-0138 (2015).
31. Antonia, S. J. *et al.* Durvalumab after chemoradiotherapy in stage III non-small-cell lung cancer. *N. Engl. J. Med.* **377**, 1919–1929. https://doi.org/10.1056/NEJMoa1709937 (2017).
32. Shaverdian, N. *et al.* Previous radiotherapy and the clinical activity and toxicity of pembrolizumab in the treatment of non-small-cell lung cancer: A secondary analysis of the KEYNOTE-001 phase 1 trial. *Lancet Oncol.* **18**, 895–903. https://doi.org/10.1016/S1470-2045(17)30380-7 (2017).
33. Kwon, E. D. *et al.* Ipilimumab versus placebo after radiotherapy in patients with metastatic castration-resistant prostate cancer that had progressed after docetaxel chemotherapy (CA184-043): A multicentre, randomised, double-blind, phase 3 trial. *Lancet Oncol.* **15**, 700–712. https://doi.org/10.1016/S1470-2045(14)70189-5 (2014).

34. Luke, J. J. *et al.* Safety and clinical activity of pembrolizumab and multisite stereotactic body radiotherapy in patients with advanced solid tumors. *J. Clin. Oncol.* **36**, 1611–1618. https://doi.org/10.1200/JCO.2017.76.2229 (2018).
35. Eikawa, S. *et al.* Immune-mediated antitumor effect by type 2 diabetes drug, metformin. *Proc. Natl. Acad. Sci. USA* **112**, 1809–1814. https://doi.org/10.1073/pnas.1417636112 (2015).
36. Hirayama, T. *et al.* Metformin prevents peritoneal dissemination via immune-suppressive cells in the tumor microenvironment. *Anticancer Res.* **39**, 4699–4709. https://doi.org/10.21873/anticanres.13652 (2019).
37. Chiang, C. F. *et al.* Metformin-treated cancer cells modulate macrophage polarization through AMPK-NF-kappaB signaling. *Oncotarget* **8**, 20706–20718. https://doi.org/10.18632/oncotarget.14982 (2017).
38. Wang, J. C. *et al.* Metformin's antitumour and anti-angiogenic activities are mediated by skewing macrophage polarization. *J. Cell Mol. Med.* https://doi.org/10.1111/jcmm.13655 (2018).
39. Uehara, T. *et al.* Metformin induces CD11b+-cell-mediated growth inhibition of an osteosarcoma: Implications for metabolic reprogramming of myeloid cells and anti-tumor effects. *Int. Immunol.* **31**, 187–198. https://doi.org/10.1093/intimm/dxy079 (2019).
40. Cha, J. H. *et al.* Metformin promotes antitumor immunity via endoplasmic-reticulum-associated degradation of PD-L1. *Mol Cell* **71**, 606-620 e607. https://doi.org/10.1016/j.molcel.2018.07.030 (2018).
41. Han, Y. *et al.* Metformin reverses PARP inhibitors-induced epithelial-mesenchymal transition and PD-L1 upregulation in triple-negative breast cancer. *Am. J. Cancer Res.* **9**, 800–815 (2019).
42. Xue, J. *et al.* Metformin suppresses cancer cell growth in endometrial carcinoma by inhibiting PD-L1. *Eur. J. Pharmacol.* **859**, 172541. https://doi.org/10.1016/j.ejphar.2019.172541 (2019).
43. Zhang, Z. *et al.* Metformin enhances the antitumor activity of CD8(+) T lymphocytes via the AMPK-miR-107-Eomes-PD-1 pathway. *J. Immunol.* **204**, 2575–2588. https://doi.org/10.4049/jimmunol.1901213 (2020).
44. Meng, F., Song, L. & Wang, W. Metformin improves overall survival of colorectal cancer patients with diabetes: A meta-analysis. *J. Diab. Res.* **2017**, 5063239. https://doi.org/10.1155/2017/5063239 (2017).
45. Ki, Y. J. *et al.* Association between metformin use and survival in non-metastatic rectal cancer treated with a curative resection: A nationwide population study. *Cancer Res. Treat.* **49**, 29–36. https://doi.org/10.4143/crt.2016.128 (2017).
46. Huang, W. K. *et al.* Postdiagnostic metformin use and survival of patients with colorectal cancer: A nationwide cohort study. *Int. J. Cancer* **147**, 1904–1916. https://doi.org/10.1002/ijc.32989 (2020).
47. Saito, A. *et al.* Metformin changes the immune microenvironment of colorectal cancer in patients with type 2 diabetes mellitus. *Cancer Sci.* **111**, 4012–4020. https://doi.org/10.1111/cas.14615 (2020).
48. Sogawa, C. *et al.* Gel-Free 3D tumoroids with stem cell properties modeling drug resistance to Cisplatin and Imatinib in metastatic colorectal cancer. *Cells* https://doi.org/10.3390/cells10020344 (2021).
49. Tsukui, H. *et al.* CD73 blockade enhances the local and abscopal effects of radiotherapy in a murine rectal cancer model. *BMC Cancer* **20**, 411. https://doi.org/10.1186/s12885-020-06893-3 (2020).
50. Formenti, S. C. & Demaria, S. Systemic effects of local radiotherapy. *Lancet Oncol.* **10**, 718–726. https://doi.org/10.1016/S1470-2045(09)70082-8 (2009).
51. Barcellos-Hoff, M. H., Park, C. & Wright, E. G. Radiation and the microenvironment: Tumorigenesis and therapy. *Nat. Rev Cancer* **5**, 867–875. https://doi.org/10.1038/nrc1735 (2005).
52. Lugade, A. A. *et al.* Local radiation therapy of B16 melanoma tumors increases the generation of tumor antigen-specific effector cells that traffic to the tumor. *J. Immunol.* **174**, 7516–7523. https://doi.org/10.4049/jimmunol.174.12.7516 (2005).
53. Gupta, A. *et al.* Radiotherapy promotes tumor-specific effector CD8+ T cells via dendritic cell activation. *J. Immunol.* **189**, 558–566. https://doi.org/10.4049/jimmunol.1200563 (2012).
54. Heylmann, D., Rodel, F., Kindler, T. & Kaina, B. Radiation sensitivity of human and murine peripheral blood lymphocytes, stem and progenitor cells. *Biochim. Biophys. Acta* **121–129**, 2014. https://doi.org/10.1016/j.bbcan.2014.04.009 (1846).
55. Xia, W. *et al.* Metformin promotes anticancer activity of NK cells in a p38 MAPK dependent manner. *Oncoimmunology* **10**, 1995999. https://doi.org/10.1080/2162402X.2021.1995999 (2021).
56. Gabrilovich, D. I. Myeloid-derived suppressor cells. *Cancer Immunol. Res.* **5**, 3–8. https://doi.org/10.1158/2326-6066.CIR-16-0297 (2017).
57. Vanhaver, C., van der Bruggen, P. & Bruger, A. M. MDSC in mice and men: Mechanisms of immunosuppression in cancer. *J. Clin. Med.* https://doi.org/10.3390/jcm10132872 (2021).
58. Li, H., Han, Y., Guo, Q., Zhang, M. & Cao, X. Cancer-expanded myeloid-derived suppressor cells induce anergy of NK cells through membrane-bound TGF-beta 1. *J. Immunol.* **182**, 240–249. https://doi.org/10.4049/jimmunol.182.1.240 (2009).
59. Hoechst, B. *et al.* Myeloid derived suppressor cells inhibit natural killer cells in patients with hepatocellular carcinoma via the NKp30 receptor. *Hepatology* **50**, 799–807. https://doi.org/10.1002/hep.23054 (2009).
60. Stiff, A. *et al.* Nitric oxide production by myeloid-derived suppressor cells plays a role in impairing Fc receptor-mediated natural killer cell function. *Clin. Cancer Res.* **24**, 1891–1904. https://doi.org/10.1158/1078-0432.CCR-17-0691 (2018).
61. Ostrand-Rosenberg, S., Sinha, P., Beury, D. W. & Clements, V. K. Cross-talk between myeloid-derived suppressor cells (MDSC), macrophages, and dendritic cells enhances tumor-induced immune suppression. *Semin. Cancer Biol.* **22**, 275–281. https://doi.org/10.1016/j.semcancer.2012.01.011 (2012).
62. Kepp, O. *et al.* Consensus guidelines for the detection of immunogenic cell death. *Oncoimmunology* **3**, e955691. https://doi.org/10.4161/21624011.2014.955691 (2014).
63. Sakata, K. *et al.* Establishment and characterization of high- and low-lung-metastatic cell lines derived from murine colon adenocarcinoma 26 tumor line. *Jpn. J. Cancer Res.* **87**, 78–85. https://doi.org/10.1111/j.1349-7006.1996.tb00203.x (1996).

Acknowledgements

This study was supported by Japan Society for the Promotion of Science (17K10649, 19K09225) in animal experiments. This study was also supported by Keirin Race Fund from JKA foundation in flowcytometric analysis using LSRFortessa. We greatly thank Ms. H. Hayakawa for her excellent technical assistance of flowcytometric analysis and Dr K. Oguri for providing LuM-1. We also thank J. Shinohara, H. Hatakeyama, N. Nishiaki and I. Nieda for technical and clerical works.

Author contributions

M.T, H.M, K.K, H.H and J.K. Conceived and designed the experiments. M.T, H.M, H.T, Y.K, Y.K, H.O, H.Y and K.Y performed the experiments. A.K.L, N.S, and J.K wrote the main manuscript. All authors reviewed the manuscript.

Competing interests

The authors declare no competing interests.

Additional information

Supplementary Information The online version contains supplementary material available at https://doi.org/10.1038/s41598-022-11236-2.

Correspondence and requests for materials should be addressed to J.K.

Reprints and permissions information is available at www.nature.com/reprints.

Publisher's note Springer Nature remains neutral with regard to jurisdictional claims in published maps and institutional affiliations.